BioMetals (2005) 18:255–267
DOI 10.1007/s10534-005-1538-3

Kinetics of the early subcellular distribution of cadmium in rat hepatocytes

Pham T.N. Diep[1], Francine Denizeau[1,†], & Catherine Jumarie[2,*]
[1]*Département de chimie;* [2]*des Sciences Biologiques, Université du Québec à Montréal, C.P. 8888, Succ. centre-ville, Montréal, Québec, Canada H3C 3P8;*Author for correspondence (Tel.: +514-987-3000, ext. 7680; Fax: +514-987-4647; E-mail: jumarie.catherine@uqam.ca)*

Received 13 October 2004; accepted 1 February 2005; Published online: March 2005

Key words: cadmium, hepatocytes, metallothionein, mitochondria, nuclei, plasma membrane, subcellular distribution

Abstract

The kinetics of the early subcellular distribution of cadmium (Cd) was characterized in primary cultures of rat hepatocytes exposed to 10, 50 and 100 μM Cd in a serum-free WME medium for 10, 30 or 60 min. Our results demonstrate a time- and concentration-dependent increase in Cd content with the highest metal concentration measured in the cytosol, whereas the lowest was observed in the mitochondria. With the exception of early localization in the plasma membrane, Cd concentrations in fractions were characterized by the following decreasing order of magnitude: cytosol > low density molecules $\sim$ nuclei > lysosomes $\sim$ mitochondria. We also found evidence for: (i) a two-step process for Cd distribution in the nuclei and mitochondria; and (ii) a time-dependent 'slow' process of transfer from the plasma membrane to the cytosol. Saturation in Cd uptake was observed at 50 μM in most cell fractions at 10 and 30 min, except for the plasma membrane. The lack of apparent saturation for Cd accumulation at 60 min was not related to an increase in metallothionein synthesis. Altogether, our data provide insights into the dynamics of transfer between intracellular compartments, and allow a better identification of the organelles that are the most subjected to Cd toxicity for early exposure conditions.

Introduction

Cadmium (Cd) is a highly toxic metal with many industrial uses that can contribute to a well-defined spectrum of diseases in animal models as well as in humans (Goering *et al.* 1995). Studies with rodents have demonstrated that following acute exposure to Cd, the preponderance of the dose accumulates in the liver, resulting primarily in liver damage (Tzirogiannis *et al.* 2003). The acute and long-term toxic effects of Cd have been described by many authors and a variety of mechanisms have been characterized for Cd-induced cytotoxicity in liver cells, including generation of reactive oxygen species, lipid peroxidation (Andersen & Andersen 1988; Shaikh *et al.* 1999), and interference with the intracellular signaling network as well as gene regulation at multiple levels (Beyersmann & Hechtenberg 1997). One of the earliest morphological changes observed in rat liver after hepatotoxic doses of Cd include the dilation of the rough endoplasmic reticulum with a loss of ribosomes, nuclear condensation, and an increase in the number of perichromatin granules (Dudley *et al.* 1984). The critical targets of Cd binding are the thiol groups of proteins. Sulfhydryl group inactivation of just a few essential proteins could produce a myriad of functional deficits in subcellular organelles, such as nuclei, mitochondria, and the endoplasmic reticulum. In addition, cytoskeletal

[†]Deceased March 25, 2004.

proteins such as tubulin contain several cysteine residues, and Cd binding to these sulfhydryls has been shown to result in disruption of cytoskeletal organization (Chou 1989; Li *et al.* 1994).

Cadmium induces the expression of several stress response genes including heat-shock proteins, metallothionein (MT), glutathione as well as other oxidative stress response elements (for review see Koizumi & Yamada 2003). MTs, first reported as Cd-binding proteins in horse kidneys (Margoshes & Vallee 1957), are ubiquitous low molecular (6–7 kDa) cysteine-rich intracellular proteins that bind with high affinity 7–12 atoms of metal ions per molecule through thiolate bridges. Metallothionein synthesis is rapidly and dramatically upregulated in response to a myriad of substances including glucocorticoids, interleukins, growth factors and stress in addition to metals (Andrews 1990). Metallothionein synthesis upregulation protects against Cd cytotoxicity: both *in vivo* and *in vitro* studies have led to the conclusion that the more MT is synthesized, the less the liver cells are sensitive to Cd-induced injuries (Cherian 1980; Goering & Klaassen 1983; Liu *et al.* 1991). In the early 1980s, it was suggested that in addition to its commonly proposed detoxification role, MT may be involved in metal storage or transport (Danielson *et al.* 1982). Today, MT proteins are believed to play a significant role in the maintenance of trace element homeostasis and in the scavenging of free radicals in addition to the detoxification of metals (Davis & Cousins 2000). Four MT isoforms have been identified to date (Palmiter 1998), but MT-1 and MT-2 are the most widely distributed isoforms (Andrews 1990). Recently, it has been proposed that liver MT-1 would be involved in the detoxification of toxic metals such as Cd, whereas MT-2 would be responsible for the homeostasis of essential metals such as Cu and Zn (Nakamura *et al.* 2004).

The role of MT in the organ distribution of Cd has been extensively studied for decades. The use of transgenic mice has allowed a better estimation of the extent to which MT may influence the organ distribution of metals: similar liver/kidney tissue content ratios have been estimated for Cd in MT-/- and wild type mice (Conrad *et al.* 1997; Liu *et al.* 2001). At the subcellular level, Cd distribution has also been studied in relation to specific toxic effects and MT expression. In liver and kidney cells, Cd is generally found to be located in the cytosolic fraction, and mainly, but not totally bound to MT (Nordberg *et al.* 1994; Wolstowski & Krasowska 1999). Cadmium also distributes in the mitochondria and the microsomal fractions as well as in the nuclei of both liver and kidney cells (Waku 1984; Rau *et al.* 1987). In accordance with its protective role against Cd-induced injury, MT has been shown to affect its subcellular distribution: Cd localization in the cytosol was promoted in rat hepatocytes pretreated with Cd to induce MT synthesis with a concomitant decrease in nuclei, mitochondria and endoplasmic reticulum Cd content (Goering & Klaassen 1983). A significant level of cytosolic Cd has also been found to be associated with high-molecular-weight proteins in rat hepatocytes, and the upregulation of MT synthesis dramatically shifts this intracellular pool of Cd to the low-molecular-weight protein fraction (Liu *et al.* 1991). Most of these studies were conducted with limited exposure conditions in control or metal-pretreated hepatocytes. Very few data are available on the very early subcellular distribution of Cd as a function of time and concentration of exposure. The aim of the present study was: (i) to characterize the kinetics of Cd accumulation in subcellular compartments as a function of time; and (ii) to determine how much the kinetics may vary with the metal concentration.

Materials and methods

Chemicals

All culture ware was from Sarstedt Inc. (Newton, NC). Minimum Essential Medium (MEM), Leibovitz 15 (L-15) medium and gentamycin were purchased from Gibco BRL (Grand Island, NY), whereas Williams' medium E (WME) was from Sigma Chemical Co. (St. Louis, MO). Fetal bovine serum (FBS) was obtained from Medicorp Inc. (Montreal, QC, Canada). Insulin, bovine serum albumin (BSA) and a mixture of protease inhibitors (Cat # P8340 containing AEBSF, aprotinin, leupeptin, bestatin, pepstatin A and E-64) were purchased from Sigma Chemical Co. ^{109}Cd-labeled $CdCl_2$ (sp. act. 1.6 mCi/mg) was purchased from PerkinElmer Life Sciences Inc. (Boston, MA). All other chemicals used for buffer preparation were

ACS reagent grade or of the highest purity commercially available. Specific reagents are described below.

Hepatocyte isolation and cell culture

The hepatocytes were isolated from male Sprague–Dawley rats (Charles River Laboratories, Wilmington, MA) weighing 140–180 *g* (around 6-weeks old) by a modification of the two-step collagenase perfusion method of Seglen (1976). The hepatocytes were purified by isodensity Percoll centrifugation, and cell viability was determined by propidium iodine (Invitrogen-Life Technologies, Burlington, ON, Canada) exclusion assay (2 μg PI/ml phosphate buffer) using flow cytometry (Becton Dickingson). Only cell preparations for which the viability was higher than 85% were used. Isolated hepatocytes were plated on collagen-coated Petri dishes at a density of 10^5 viable cells/cm^2 in WME containing 0.2 μM bovine insulin, 50 μg/ml gentamycin, and supplemented with 10% FBS. Cultures were maintained at 37 °C in a humidified 5% CO_2-air atmosphere. Following a 2-h incubation, the cultures were washed with serum-free MEM and were then kept in L-15 medium for 20 h before being used for subsequent experiments.

Subcellular fractionation

Twenty-hours old cell cultures were washed two times with 8 ml (100 mm diameter Petri dishes) of MEM medium before exposure to 10, 50 or 100 μM Cd for 10, 30 and 60 min in the serum-free WME medium. After the treatment, the cells were washed twice with 8 ml buffer A (250 mM sucrose, 20 mM HEPES, 0.01 mg/ml of the protease inhibitor cocktail, pH 7.4), carefully scraped off the dishes with a rubber policeman, and resuspended in 1 ml of ice-cold buffer A. For each experimental condition, cells from three Petri dishes were pooled to get enough material and were then homogenized with a potter (Kontes Glass Co., DUALL® 22). The fractionation method used in this study is an adaptation of the method used by Simpson *et al.* (1983) and has been described previously (Messer & Lucas 2002). Briefly, the homogenates were centrifuged at 1500 *g* for 5 min to remove intact cells, and the resulting supernatants were then centrifuged at 16 000 *g* for 20 min (Hitachi SCP 70H Ultracentrifuges). The pellets, which contained membrane fragments and nuclei, were resuspended in buffer B (20 mM HEPES, 0.01 mg/ml of the protease inhibitor cocktail, pH 7.4) and applied to a sucrose cushion (1.12 M sucrose) and then centrifuged at 100 000 *g* for 60 min (Beckman Optima™ TLX Ultracentrifuge). The tops of the cushions were removed, resuspended in buffer B and then centrifuged at 30 000 *g* for 30 min. The resulting pellets contained plasma membranes. In parallel, the parts below the cushion were also collected and centrifuged at 1000 *g* for 10 min to obtain the nuclei (the resulting pellets) and the mitochondria (supernatants). The supernatants that were obtained after centrifuging the initial cell lysate (16 000 *g* for 20 min) were sampled and centrifuged at 30000 *g* for 30 min. The resulting pellets were the lysosomic fractions (Wells *et al.* 1987). The supernatants were subjected to a centrifugation at 25 0000 *g* for 90 min; the resulting pellets and supernatants contained the low density molecules (LDM) and the cytosol, respectively. Note that EDTA was omitted from the original protocol to avoid excess metal extraction by chelation and to minimize metal loss during fractionation. All steps of the fractionation procedure were undertaken at 4 °C. Samples of subcellular fractions were analyzed for protein determination using the Micro BCA™ protein Assay Reagent Kit (Pierce, Rockford, IL, USA) and bovine serum albumin as the calibration standard. Samples were then stored at −80 °C until analyzed for Cd content.

Cadmium content determination in subcellular fractions

Subcellular fractions were wet-ashed in HNO_3 (u.p.) (BDH, Toronto, ON, Canada)-H_2O_2 and Cd contents were determined by graphite furnace atomic absorption spectrometry (Manca *et al.* 1992) using a 906-AA atomic absorption spectrometer equipped with a GF 3000 graphite tube atomizer and a PAL 2000 programmable autosampler (GBC Scientific Equipment). To avoid Cd contamination, all glassware was acid-washed (in 10% HNO_3 and immediately rinsed in distilled and double deionized water) and blanks were run along with the samples. The Cd stock solution used for the calibration standard (ppb levels, i.e.,

pg Cd/ml) was prepared from an atomic absorption standard solution containing 1010 μg Cd/ml in 1% HNO_3, which matches the final acid concentration in the digested samples. Five microlitres of each sample were used for Cd content determination which was then normalized for protein content in 5 μl; the Cd contents in each fraction are thus expressed as pg Cd/mg protein of the fraction.

Isolation of total RNA

All solutions, glassware and water used for RNA isolation were made RNase-free by treating them with 0.1% diethyl pyrocarbonate (DEPC) and autoclaving. For each experimental condition, cells from two Petri dishes (100 mm diameter) were pooled to get enough material. Total RNA was extracted from the hepatocytes using TRIZOL® reagent (Invitrogen-Life Technologies, Burlington ON, Canada), according to the supplier's instructions. The RNA pellets were dried and then dissolved in 30–50 μl DEPC-treated water. The purity and concentration of the samples were assessed spectrophotometrically (Beckman DU®650) at 260 and 280 nm (260–280 nm absorbance ratios higher than 1.7 were considered as acceptable, whereas 1 unit of A_{260} was equivalent to 40 μg RNA). In addition, RNA integrity was verified by the presence of ribosomal RNA (ethidium bromide staining of the 18S and 28S bands) following agarose gel electrophoresis.

Reverse transcription and polymerase chain reaction of MT-1 and MT-2 cDNA (RT-PCR)

The levels of mRNA MT-1 and MT-2 were estimated by semi-quantitative RT-PCR using the SuperScript™ One-Step RT-PCR with Platinum® *Taq* System Kit (Invitrogen-Life Technologies). The RT-PCR method was carried out as previously reported (Ren *et al.* 2003) with minor modifications. The sense and antisense primer sequence for the rat MT-1, MT-2, and β-actin (using as an internal control) were 5′-ACTGCCTTCTTGTCG CTTA-3′ and 5′-TGGAGGTGTACGGCAAGA CT-3′; 5′-CCAACTGCCGCCTCCATTCG-3′ and 5′-GAAAAAAGTGTGGAGAACCG-3′; 5′-CCC ATTGAACACGGCATTG-3′ and 5′-GGTACG-ACCAGAGGCATACA-3′, respectively (synthesized at the Sheldon Biotechnology Centre, McGill University, Montreal, QC, Canada). The primers amplify a fragment of 310, 300 and 236 pb for MT-1, MT-2, and β-actin, respectively. RT-PCR was carried out with 1 μg of total RNA in 50 μl of reaction mixture according to the instructions of the supplier and using the GeneAmp® PCR System 9700 (Applied Biosystems, Streetsville, ON, Canada). RT-PCR was initiated by cDNA synthesis at 50 °C for 30 min and pre-denaturation was carried out at 94 °C for 1 min, followed by 27 cycles consisting of: denaturation at 94 °C for 1 min, annealing at 55 °C for 1 min, and extension at 72 °C for 1 min. A final extension step at 72 °C for 5 min was added. In order to guarantee amplification in phase of exponential increase, we minimized the cycles of PCR in condition that the strap of gel electrophoresis can be detected (data not shown). The PCR products were resolved on 2.0% (w/v) agarose gels containing 0.05 μg/ml ethidium bromide and visualized under UV *trans*-illumination using a Chemilmager™5500 Fluorescence system controlled by AlphaEase FC™ software (Alpha Innotech Corporation). MTs and actin bands were marked, set at the same width, and the total band areas were subjected to densitometry scanning. The expression of MT mRNA was normalized to β-actin.

Detection of MT protein by Western blotting

MT protein was detected by Western blot analysis using a modified procedure of Mizzen *et al.* (1996) more recently described by Perez and Cederbaum (2003). Briefly, the hepatocytes from two Petri dishes were washed twice with 8 ml phosphate-buffered saline (PBS), pooled together and then homogenized in the ice-cold buffer containing 10 mM Tris–HCl, 5 mM EDTA, 0.01 mg/ml of the protease inhibitor cocktail, pH 7.0, with the PTA 7 K1 probe of a polytron (model PCU 11, Brinkmann Instruments). Homogenates were centrifuged at 20000 *g* for 45 min at 4 °C (Hitachi SCP 70H Ultracentrifuges). Cell lysates (100 μg of total protein) were diluted 1:1 with sample buffer [10 mM Tris–HCl, 10 mM EDTA, 20% (v/v) glycerol, 1% (w/v) SDS, 0.005% (w/v) bromophenol blue, and 100 mM dithiothreitol] and then separated in an 18% polyacrylamide gel. Transfer to nitrocellulose membranes (Bio-Rad) was performed in a Bio-Rad mini-gel blotting apparatus at 40 V for 1 h using the transfer buffer:

10 mM 3-cyclohexylamino-1-propanesulfonic acid, 2 mM $CaCl_2$, and 10% methanol, pH 10.8, followed by membrane incubation in 2.5% glutaraldehyde in water for 1 h. The membranes were washed three times for 10 min in PBS; 50 mM monoethanolamine was added to the third wash solution to quench residual glutaraldehyde reactivity. The membranes were blocked in 3% BSA in Tris-buffered saline (TBS) for 2 h at room temperature and then incubated with mouse anti-metallothionein monoclonal antibody (SPA-550, StressGen, Victoria, British Columbia, Canada) diluted 1:600 in 2% BSA in TBS, overnight at room temperature. After this period of incubation, the membranes were washed with TBS-Tween 20 (0.1%) (Sigma), and incubated with Horseradish Peroxidase-conjugated antimouse antisera (Amersham Pharmacia Biotech, Buckinghamshire, England) at a dilution of 1:1000 in 2% BSA in TBS for 4 h at room temperature. Blots were washed with TBS-Tween 20 and then detected by the chemiluminescence reaction using the ECL Reagent Plus kit (PerkinElmer, Life Sciences, Boston, MA). Purified MT (containing both MT-1 and MT-2) from rabbit liver (Sigma) was used as a standard to verify antibody specificity (data not shown).

Statistical analysis

Data are presented as mean ± SD evaluated on three different cell preparations. Statistical analyses were performed with the two-tailed *t* test for unpaired data on small samples with Welch's correction using InStat software (GraphPad Software). Statistical significance was assessed at the $P < 0.05$ level.

Results

Kinetics of the early subcellular distribution of Cd

Figure 1 shows the time-course of subcellular distribution of Cd in hepatocytes following metal uptake under similar exposure conditions. A time-dependent increase in Cd content was observed for most cellular compartments with the following particularities: an equilibrium of accumulation was observed in the nuclei and mitochondria following a 30-min exposure to 10 μM Cd

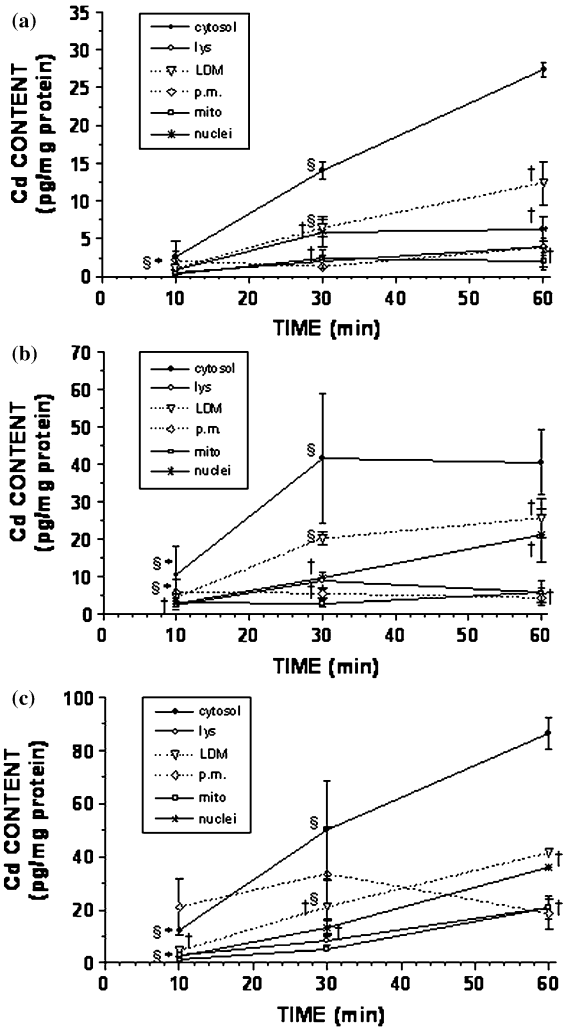

Figure 1. The time-course of subcellular distribution of Cd was measured by atomic absorption spectrometer as described in 20-h-old rat hepatocytes exposed to 10 μM (a), 50 μM (b) or 100 μM (c) Cd in serum-free WME medium. Subcellular fractions shown are lys: lysosomes; LDM: low-density macromolecules; p.m.: plasma membrane; mito: mitochondria; in addition to the cytosol and nuclei fractions. Data shown are the means ± SD evaluated for three different hepatocyte preparations. * and § indicate significant differences ($P < 0.05$) compared to Cd content measured at 30 and 60 min, respectively (same subcellular distribution). † indicates significant differences ($P < 0.05$) with cytosolic content (same exposure time).

(Figure 1a); equilibrium of accumulation was no longer observed in these organelles when cells were exposed to 50 μM Cd, but metal uptake clearly plateaued in the cytosol and LDM fractions (Figure 1b); in all subcellular compartments of cells exposed to 100 μM Cd, except the plasma

membrane, metal accumulated with no evidence of any plateau (Figure 1c). Note that in Figure 1, Cd contents are expressed relative to the protein of the subcellular fraction of concern, rather than to the total protein of the cell lysate. Therefore, the data are more representative of the Cd concentration in each subcellular compartment rather than the contribution of each compartment to the total cellular Cd.

Because of the unequal amounts of homogenate used at each step of the fractionation procedure, the percentage of total Cd recovered in a given fraction was not estimated. However, data of Cd content in each subcellular compartment expressed relative to cytosolic content allows a good estimation of how Cd distributes among fractions. Figure 2 reveals that Cd concentration in lysosomes and the LDM fraction increased proportionally to the cytosolic content as a function of time and level of exposure. It is noteworthy that the relative plasma membrane content decreased as a function of time regardless of the exposure concentration. Also, increases in the mitochondria and the nuclei contents as a function of time and relative to cytosol were observed only at 50 μM and 100 μM Cd. At 10 μM, Cd does not distribute in these organelles as much as in the cytosol at 60 min. With the exception of the early distribution at the plasma membrane, the Cd concentration in fractions was characterized by the following decreasing order of magnitude: cytosol > low density molecules $\sim$ nuclei > lysosomes $\sim$ mitochondria.

As shown in Figure 3, a concentration-dependent increase in Cd accumulation was also observed. In all cellular fractions, except the plasma membrane, saturation of accumulation was obvious at 50μM Cd for both the 10-min and the 30-min exposure times (Figure 3a, b). Interestingly, no saturation was detected for the 60-min accumulation levels, regardless of the subcellular component (Figure 3c).

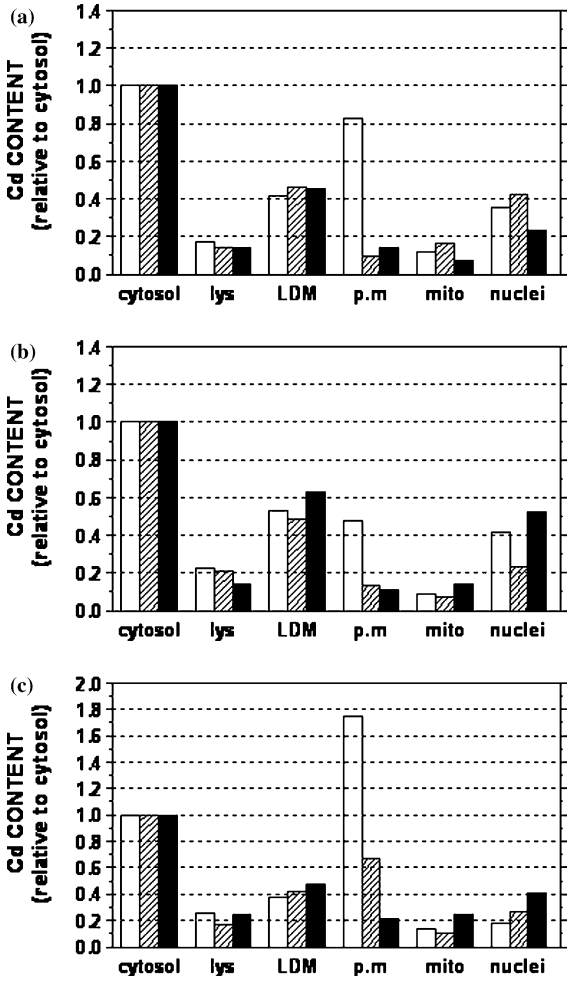

Figure 2. Subcellular distribution of Cd in 20-h-old rat hepatocytes relative to cytosolic content. Experimental conditions were as described in the legend to Figure 2 showing Cd content (pg/mg protein) in each subcellular fraction following a 10-min (open columns), 30-min (dashed columns) or 60-min (filled columns) exposure to 10 μM (a), 50 μM (b), or 100 μM (c) Cd added to serum-free WME medium. Data shown are the means evaluated for three different hepatocyte preparations. Error bars are omitted for simplicity.

mRNA levels of MTs following exposure to Cd

mRNA expression of both MT-1 and MT-2 genes in Cd-treated rat hepatocytes was evaluated by semi-quantitative RT-PCR analysis. A representative RT-PCR amplification of MT-1 (A) and MT-2 (B) mRNAs as a function of time of exposure to 10, 50 and 100 μM Cd is shown in Figures 4, 5 and 6, respectively. MTs/β-actin mRNA ratios were also estimated by densitometry analysis as a function of time (c in Figures 4–6). Untreated hepatocytes expressed relatively high basal levels of mRNA of both MT isoforms with similar MTs/β-actin mRNA ratios: 0.6 for MT-1; 0.5 for MT-2. These ratios measured in different cell preparations were highly reproducible (compare control values in Figures 4–6).

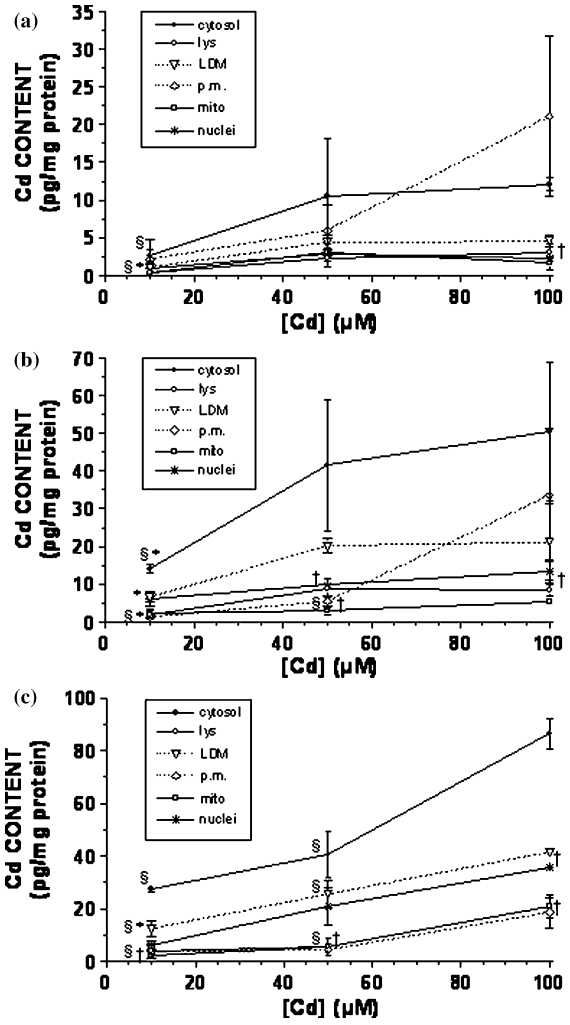

Figure 3. The subcellular distribution of Cd was measured by atomic absorption spectrometer in 20-h-old rat hepatocytes following a 10-min (a), 30-min (b) or 60-min (c) exposure to increasing concentration of Cd in the serum-free WME medium. Subcellular fractions shown are lys: lysosomes; LDM: low-density macromolecules; p.m: plasma membrane; mito: mitochondria; in addition to the cytosol and nuclei fractions. Data shown are the means ± SD evaluated on three different hepatocyte preparations. * and § indicate significant differences ($P < 0.05$) compared to Cd content measured at 50 and 100 μM, respectively (same subcellular distribution). † indicates significant differences ($P < 0.05$) with cytosolic content (same exposure concentration).

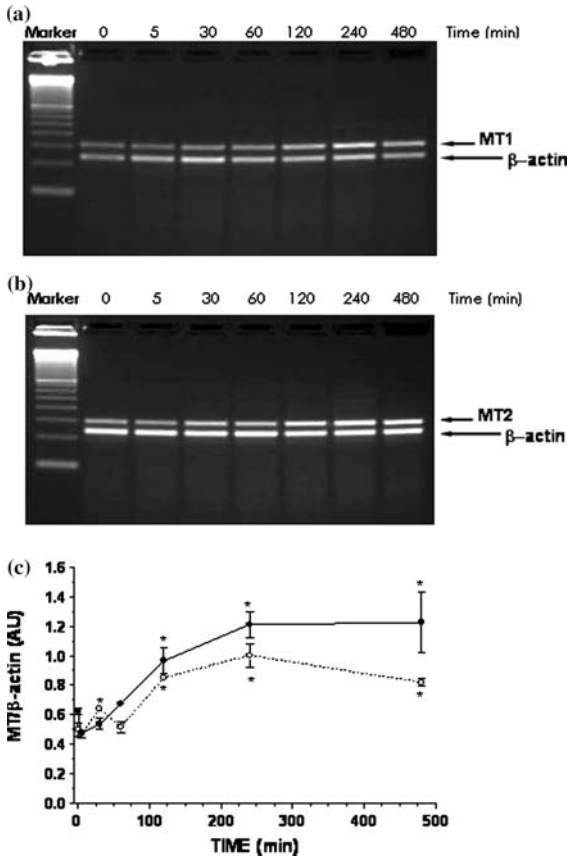

Figure 4. Representative RT-PCR amplification of MT-1 (a), MT-2 (b) and β-actin mRNAs of 20-h-old rat hepatocytes exposed to 10 μM Cd in serum-free WME medium for specific times (0–480 min). The left lanes were loaded with a molecular size marker. RT-PCR products were resolved by agarose gel electrophoresis as described in Materials and methods. Image analysis of the amplified fragments allowed the MT_1 (filled circles) and MT_2 (open circles) mRNA expression levels to be normalized to the the expression of the internal control β-actin (c). Each data represents the means ± SD evaluated for 2–4 different hepatocyte preparations. * indicates significant differences ($P < 0.05$) compared to the untreated control cells.

The time-course studies reveal that a 2-h exposure to 10 μM was required to detect a significant increase in cellular mRNA of both MT-1 and MT-2 (Figure 4). At 6 h, mRNA levels reached a plateau for MT-1 as well as for MT-2. At this time, a 93% and 100% increase in the relative mRNA level were estimated for MT-1 and MT-2, respectively. mRNA content remained constant for MT-1 up to 8 h, whereas a 18% decrease was noted for MT-2.

MTs mRNA contents in cells exposed to 50 and 100 μM were studied only over a 2-h exposure because of significant decreases in cell viability occurring for longer periods of exposure to these metal concentrations. It is noteworthy that 50 μM Cd only modified slightly the cellular mRNA levels of both MT isoforms: a 17% increase in the MT-1/β-actin mRNA ratio was observed at 1 h but this

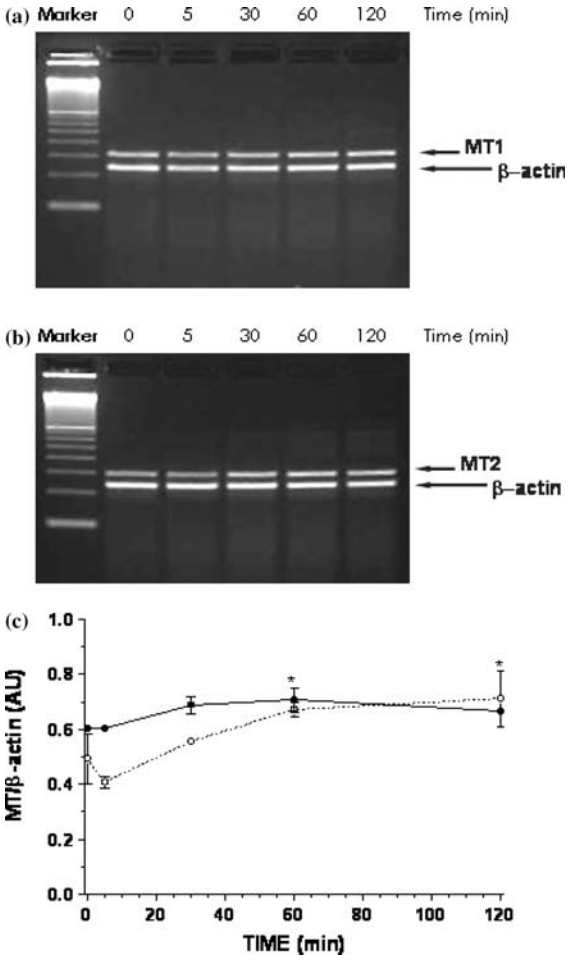

Figure 5. Representative RT-PCR amplification of MT-1 (a), MT-2 (b) and β-actin mRNAs of 20-h-old rat hepatocytes exposed to 50 μM Cd in serum-free WME medium for specific times (0–120 min). The left lanes were loaded with a molecular size marker. RT-PCR products were resolved by agarose gel electrophoresis as described in Materials and methods. Image analysis of the amplified fragments allowed the MT_1 (filled circles) and MT_2 (open circles) mRNA expression levels to be normalized to the expression of the internal control β-actin (c). Each data represents the means ± SD evaluated for 2–4 different hepatocyte preparations. *indicates significant differences ($P < 0.05$) compared to the untreated control cells.

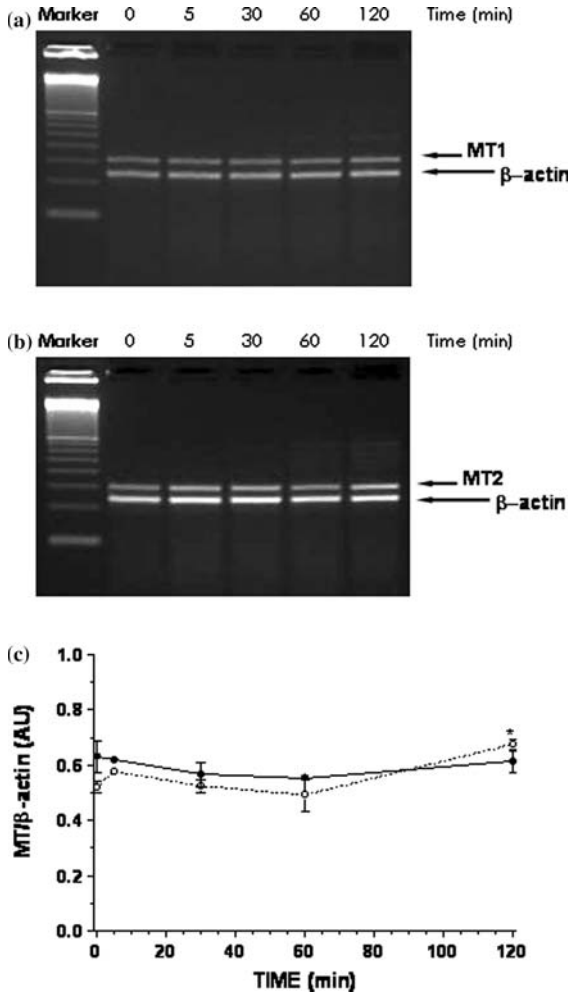

Figure 6. Representative RT-PCR amplification of MT_1 (a), MT2 (b) and β-actin mRNAs of 20-h-old rat hepatocytes exposed to 100 μM Cd in serum-free WME medium for specific times (0–480 min). The left lanes were loaded with a molecular size marker. RT-PCR products were resolved by agarose gel electrophoresis as described in Materials and Methods. Image analysis of the amplified fragments allowed the MT_1 (filled circles) and MT_2 (open circles) mRNA expression levels to be normalized to the expression of the internal control β-actin (c). Each data represents the means ± SD evaluated for 2–4 different hepatocyte preparations. *indicates significant differences ($P < 0.05$) compared to the untreated control cells.

increase was no longer observed at 2 h; a 44% increase in MT-2 mRNA level relative to β-actin was noted at 2 h (Figure 5). Similarly, 100 μM Cd did not affect MTs mRNA expression as much since only a 30% increase in MT-2/β-actin mRNA was observed at 2 h (Figure 6). Although MT-1 mRNA levels were always slightly higher than MT-2, the differences were not significant.

MT protein level following exposure to Cd

The expression of MT protein as a function of time of exposure to Cd was studied by Western blot analysis using an antibody that recognizes both MT isoforms. The blot background did not allow us to proceed with densitometry analysis,

but the representative Western blot shown in Figure 7 reveals that the MT protein level increased during the first hour of exposure to 10 μM with a tendancy to plateau from 2 to 8 h, which mimics quite well the evolution of MTs/β-actin mRNA ratio (Figure 4c). Also, as observed for mRNA, slight increases in MT protein levels were detected during the first hour of exposure to 50 μM or 100 μM with the highest protein detection at 2 h. Note that in all cases, basal MT levels measured in untreated cells were at the limit of detection.

Discussion

Broad distribution with evidence of a two-step process in mitochondria and nuclei

The use of serum-free WME medium allowed us to conduct experiments on cells exposed to Cd concentrations as high as 100 μM for up to 60 min, but longer exposure times led to significant loss in cell viability (data not shown). Our results demonstrate a time- and concentration-dependent increase in Cd content with the highest metal concentration measured in the cytosol, whereas the lowest was generally observed in the mitochondria (Figures 1–3). A number of studies have shown that Cd distributes throughout the cells. In the liver as well as the kidneys of bank voles exposed for 6 weeks to dietary Cd (40–80 μg Cd/g dry weight), Cd was mainly found in the cytosol but also in the nuclei and particulate fractions (Wlostowski & Krasowska 1999). In calves injected with 1–10 mg Cd/animal/day for 95 days, Cd in liver cells was detected in the nuclei, the mitochondria, the endoplasmic reticulum and the lysosomes (Horky *et al.* 2002). Also, a significant amount of Cd was recovered in the nuclei of rat liver as soon as 1 h after a single injection of 3 μmol Cd/Kg (Rau *et al.* 1987). Cadmium distribution in the nucleus is critical since Cd binds DNA, produces single strand DNA breaks and DNA-protein cross-links, and promotes mutagenesis (Shiraishi *et al.* 1995; Misra *et al.* 1998). Depending on the exposure conditions and the model used, Cd may also induce either apoptosis or stimulate DNA synthesis (Von Zglinicki *et al.* 1992 Lemarie *et al.* 2004). Studies using fluorescent dye have also provided evidence of the early distribution of Cd in different organelles. In canine kidney cells, Hamada *et al.* (1994) observed Cd-8-hydroxyquinoline fluorescence in the cytoplasm within 30 min and in the nuclei after 60–90 min following exposure to 100 μM $CdCl_2$. Our previous studies performed with rhodamine 123 demonstrated that Cd may disrupt the mitochondrial membrane potential in intestinal Caco-2 cells as soon as 2 min after exposure to 100 μM Cd (Bolduc *et al.* 2004). Mitochondria are now well recognized as metal-target organelles, and Cd may directly disrupt these organelles, a process that is associated with both apoptosis and

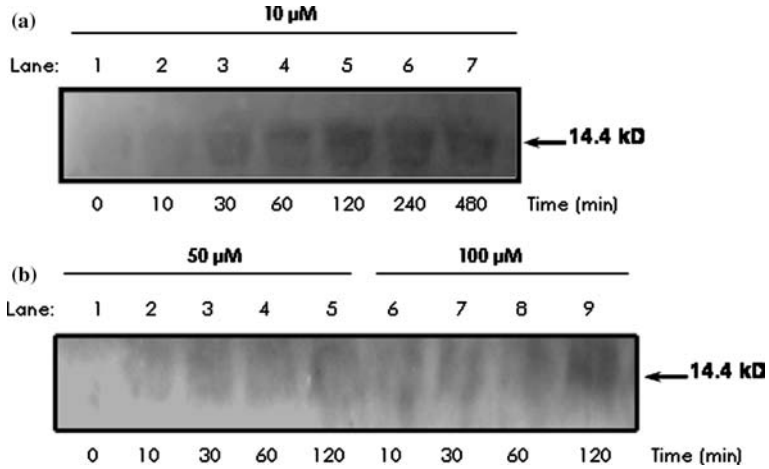

Figure 7. Metallothionein protein detection in 20-h-old primary cultures of rat hepatocytes exposed to 10 μM (a) or 50 and 100 μM (b) Cd added to serum-free WME medium. At specific time points, cell lysates were collected and analyzed by Western blot as described in Materials and methods. Metallothionein protein in untreated control cells is shown in lanes 1.

necrosis (Lemasters 1999). Oxidative stress is often cited as a plausible cause of Cd-induced hepatotoxicity, but cytosolic reactive oxygen species (ROS) formation as a prerequisite for mitochondrial membrane potential disruption has been questioned (Bolduc *et al.* 2004). Alternatively, mitochondria represent a significant site of ROS formation by non-redox or poor redox cycling transition metals (Cd^{2+}, Hg^{2+}, As^{3+}) in rat hepatocytes (Pourahmad *et al.* 2003), and Cd can have dual effects on respiratory chain activity and permeability transition (Belyaeva *et al.* 2001). Cadmium, through the generation of ROS and prior to significant cellular damage, activates the stress-related signal protein c-Jun N-terminal kinase (JNK), increases *c-jun* expression, and promotes the binding of the transcription factor of activator protein-1 (AP-1) to DNA in primary cultures of rat hepatocytes (Hsiao & Stapleton 2004).

Our present time-course studies show that cell exposure to only 10 μM Cd is sufficient to reach equilibrium of accumulation as early as 30 min in the nuclei and the mitochondria, whereas 50 μM is needed to equilibrate Cd content in the cytosol (Figure 1). Under these conditions, equilibrium in Cd content in the nuclei and mitochondria is no longer observed. At higher levels of exposure (100 μM), Cd still accumulated in all cellular fractions. Hence Cd uptake in the nuclei and the mitochondria may be characterized by a two-step process: an initial equilibrium level of accumulation is achieved 'rapidly' while Cd content still increases in the cytosol; when metal content in the cytosol equilibrates, then Cd is further distributed to the mitochondria and the nuclei. To our knowledge, transport mechanisms responsible for Cd accumulation in different organelles are still unknown but specific transport for the uptake of essential metals (Cu, Zn and Fe) in the mitochondria and the lysosomes has been characterized in numerous species and cell types (Chavez-Crooker *et al.* 2003; Guan *et al.* 2003; Li & Kaplan 2004).

Plasma membrane is an important transient pool for early cellular distribution

Another important observation from our time-course studies performed with different concentrations of Cd involves the kinetics of Cd content in the plasma membrane. Indeed, in Figure 1a and b, it is apparent that the metal content in the plasma membrane remains low compared to cytosol for the 10 and 50 μM exposure concentrations. However, Figure 2a and b clearly show that metal membrane content relative to cytosol rapidly decreases between 10 and 30 min. This phenomenon was even more pronounced at 100 μM Cd, the concentration at which the initial membrane contents measured at 10 min were 1.8-fold higher than the cytosolic levels (Figures 1c and 2c). Hence, although the cellular accumulation of Cd is considered to be 'rapid' (globally), a time-dependent 'slow' process of transfer from the plasma membrane to the cytosol becomes evident. The plasma membrane may represent an important target for Cd which is known to favor lipid peroxidation in the liver (Andersen & Andersen 1988; El-Maraghy *et al.* 2001). In renal cortical cells, a significant accumulation of Cd in the membrane fraction has also been suggested to be a critical determinant of Cd nephrotoxicity (Nordberg *et al.* 1994). Cadmium-induced disruption of liver homeostasis, including disregulation of cell proliferation, may in part be related to its presence in the plasma membrane. Gap junctional intercellular communications (GJIC) maintain cellular homeostasis at the organ level, and a time-dependent inhibition of liver GJIC has been demonstrated in mice injected with different doses of Cd (Jeong *et al.* 2000). This effect was correlated to a decrease in the expression of connexins Cx32 and Cx26 in addition to a disruption of cytoskeletal actin in the liver. Cadmium has also been shown to directly damage or indirectly affect the expression of the adhesion molecules, cadherins and NCAM (for review see Prozialeck *et al.* 2002). This possibly contributes to abnormal differentiation and malignant progression (Waisberg *et al.* 2003). The importance of membrane proteins as targets for Cd toxicity is further strengthened by our results showing no evidence of any saturation in Cd accumulation in the plasma membrane, whereas saturation was clearly observed at 50 μM Cd in all other subcellular fractions for the 10 min and the 30 min exposure times (Figure 3a and b). The plasma membrane has a relatively high capacity for the early accumulation of Cd and may represent an important transient pool for cellular Cd.

Early changes in subcellular distribution are not related to a higher level of MT expression

In the present study, we found the time-course of Cd accumulation in the LDM fraction to follow quite well the cytosolic one (Figure 1). Also, similar concentration-dependent curves were obtained for Cd accumulation in the cytosol and the LDM fraction, whether or not saturation was observed (Figure 3). Our study does not allow the contribution of MT in the total metal content in the cytosol to be estimated, but MT expression was measured. MT-1 and MT-2 genes are highly inducible in mammalian cells by many metals; the concentration of metal ions required to induce MTs, and the time required to reach peaks in transcription levels vary according to the inducing metal. MT expression has also been shown to vary with the tissue of concern but marked induction by Cd is generally observed in the liver (Zhou *et al*. 1999). It is therefore justified to ask whether the lack of equilibrium of accumulation at 100 μM Cd (Figure 1c) as well as the lack of apparent saturation at 60 min (Figure 3c) in both fractions (cytosol and LDM) could be related to higher levels of MT. Our results showing no variation in MT expression during the first hour of exposure clearly reveal that MT synthesis is not responsible for the net increases in Cd accumulation measured at 100-μM without saturation at 60 min. However, we measured a significant increase in both MT-1 and MT-2 mRNA levels following a 2-h exposure to 10 μM (Figure 4). Because of altered cell viability, experiments using higher concentrations of Cd were conducted over a 2-h exposure only. Our results led to the conclusion that increasing the Cd concentration up to 100 μM does not shorten the minimal period of time required to induced mRNA synthesis (Figures 5 and 6). Why 50 and 100 μM Cd failed to induce MTs synthesis at 2 h remains to be clarified. Although the preponderance of evidence indicates a transcriptional level of regulation for MT synthesis, some results suggest that post-transcriptional modulation is also important for MT expression since a quantitative relationship between MT mRNA and protein levels is not always observed (Vasconcelos *et al*. 2002). Our Western analysis did not allow any protein quantification but it agrees with the results obtained with RT-PCR amplification (Figure 7).

In conclusion, we have characterized the kinetics of the early subcellular distribution of Cd as a function of increasing concentrations. Our data increase our knowledge of the dynamics of transfer between intracellular compartments which should allow to better identify the organelles that are the most subjected to Cd toxicity for early exposure conditions.

Acknowledgements

This work was supported by the Natural Sciences & Engineering Research Council of Canada, NSERC (Collaborative Health Research project, grant CHR238001-00; and Discovery grant, CJ, grant RGPIN-203202). The authors thank Dr Richard Desrosier for excellent advice concerning the detection of metallothionein protein. A note of thanks to Mr Pierre Cayer for his technical assistance in Cd content analysis.

References

Andersen HR, Andersen O. 1988 Effect of cadmium chloride on hepatic lipid peroxydation in mice. *Pharmacol Toxicol* **63**, 173–177.

Andrews GK. 1990 Regulation of metallothionein gene expression. *Prog Food Nutr Sci* **14**, 193–258.

Belyaeva EA, Glazunov VV, Nikitina ER, Korotkov SM. 2001 Bivalent metal ions modulate Cd^{2+} effects on isolated rat liver mitochondria. *J Bioenerg Biomembr* **33**, 303–318.

Beyersmann D, Hechtenberg S. 1997 Cadmium, gene regulation, and cellular signaling in mammalian cells. *Toxicol Appl Pharmacol* **144**, 247–261.

Bolduc JS, Denizeau F, Jumarie C. 2004 Cadmium-induced mitochondrial membrane potential dissipation does not necessarily require cytololic oxidative stress: studies using rhodamine-123 fluorescence unquenching. *Toxicol Sci* **77**, 299–306.

Bradford MM. 1976 A rapid and sensitive method for the quantitation of microgram quantitites of protein utilizing the principle of protein-dye binding. *Anal Biochem* **72**, 248–254.

Chavez-Crooker P, Garrido N, Ahearn GA. 2003 Copper transport by lobster (*Homarus americanus*) hepatopancreatic lysosomes. *Comp Biochem Physiol* **135 C**, 107–118.

Cherian G. 1980 The synthesis of metallothionein and cellular adaptation to metal toxicity in primary rat kidney epithelial cell cultures. *Toxicology* **17**, 225–231

Chou IN. 1989 Distinct cytosqueletal injuries induced by arsenic, cadmium, cobalt, chromic, and nickel compounds. *Biomed Environ Sci* **2**, 358–365.

Conrad CC, Walter CA, Richardson A, Hanes MA, Grabowski DT. 1997 Cadmium toxicity and distribution in metallothionein-I and metallothionein-II deficient transgenic mice. *J Toxicol Environ Health* **52**, 527–543.

Danielson KG, Ohi S, Huang PC. 1982 Immunochemical detection of metallothionein in specific epithelial cells of rat organs. *Proc Natl Acad Sci USA* **79**, 2301–2304.

Davis SR, Cousins RJ. 2000 Metallothionein expression in animals: a physiological perspective on function. *J Nutr* **130**, 1085–1088.

Dudley RE, Swoboda DJ, Klaassen CD. 1984 Time course of cadmium-induced ultrastructural changes in rat liver. *Toxicol Appl Pharmacol* **76**, 50–160.

El-Maraghy SA, Gad MZ, Fahim AT, Hamdy MA. 2001 Effect of cadmium and aluminium intake on the antioxydant status and lipid peroxidation in rat tissues. *J Biochem Mol Toxicol* **15**, 207–214.

Goering PL, Waalkes MP, Klaassen CD. 1995 Toxicology of cadmium. In Goyer RA, Cherian MG, eds. *Toxicology of Metals, Biochemical Aspects*, Berlin: Springer, 189–214.

Goering PL, Klaassen CD. 1983 Altered subcellular distribution of cadmium following cadmium pretreatment: possible mechanism of tolerance to cadmium-induced lethality. *Toxicol Appl Pharmacol* **70**, 195–203.

Guan Z, Kukoyi B, Feng P, Kennedy MC, Franklin RB, Costello LC. 2003 Kinetic identification of a mitochondrial zinc uptake transport process in prostate cells. *J Inorg Biochem* **97**, 199–206.

Hamada T, Tanimoto A, Iwai S, Fujiwara H, Sasaguri Y. 1994 Cytopathological changes induced by cadmium-exposure in canine proximal tubular cells: a cytochemical and ultrastructural study. *Nephron* **68**, 104–111.

Horky D, Lauschova I, Illek J, Pechova A, Sindelar M. 2002 Distribution of exogenous heavy metals in the hepatocytes of calves: a morphometric study. *Microsc Res Tech* **56**, 451–453.

Hsiao CJ, Stapleton SR. 2004 Characterization of Cd-induced molecular events prior to cellular damage in primary rat hepatocytes in culture: activation of the stress activated signal protein JNK and transcription factor AP-1. *J Biochem Mol Toxicol* **18**, 133–142.

Jeong SH, Habeebu SS, Klaassen CD. 2000 Cadmium decreases gap junctional intercellular communication in mouse liver. *Toxicol Sci* **57**, 156–166.

Koizumi T, Shirakura H, Kumagai H, Tatsumoto H, Suzuki KT. 1996. Mechanisms of cadmium-induced cytotoxicity in rat hepatocytes: cadmium-induced active oxygen-related permeability changes of the plasma membrane. *Toxicology* **114**, 125–134.

Koizumi S, Yamada H. 2003 DNA microarray analysis of altered gene expression in cadmium-exposed human cells. *J Occup Health* **45**, 331–334.

Lemarié A, Lagadic-Gossmann D, Morzadec C, Allain N, Fardel O, Vernhet L. 2004 Cadmium induces caspase-independent apoptosis in liver Hep3B cells: role for calcium in signalling oxidative stress-related impairment of mitochondria and relocation of endonuclease G and apoptosis-inducing factor. *Free Radic Biol Med* **36**, 1517–1531.

Lemasters JJ. 1999 Mechanisms of hepatic toxicity: part V. Necrapoptosis and the mitochondrial permeability transition: shared pathways to necrosis and apoptosis. *Am J Physiol Gastrointest Liver Physiol* **276**, G1–G6.

Li L, Kaplan J. 2004 A mitochondrial-vacuolar signaling pathway in yeast that affects iron and copper metabolism. *J Biol Chem* **279**, 33651–33661.

Li W, Kagan HM, Chou IN. 1994 Alterations in cytoskeletal organization and homeostasis of cellular thiols in cadmium-resistant cells. *Toxicol Appl Pharmacol* **126**, 114–123.

Liu J, Kershanw WC, Klaassen CD. 1991 The protective effect of metallothionein on the toxicity of various metals in rat primary hepatocyte culture. *Toxicol Appl Pharmacol* **107**, 27–34.

Liu Y, Liu J, Klaassen CD. 2001 Metallothionein-null and wild type mice show similar cadmium absorption and tissue distribution following oral cadmium administration. *Toxicol Appl Pharmacol* **175**, 253–259.

Manca D, Lefevre M, Trottier B, *et al*. 1992 Micro method for determination of cadmium in tissues and slurried samples by use of flameless atomic absorption spectrometry. *Microchem J* **46**, 249–258.

Margoshes M, Vallee BL. 1957 A cadmium protein from equine kidney cortex. *J Am Chem Soc* **79**, 4813–4814.

Messer RLW, Lucas LC. 2002 Localization of metallic ions within gingival fibroblast subcellular fractions. *J Biomed Mater Res* **59**, 466–472.

Misra RR, Page JE, Smith GT, Waalkes MP, Dipple A. 1998 Effect of cadmium exposure on background and anti-5 methylchrysene-1,2-dihydrodiol 3,4-epoxide-induced mutagenesis in the supF gene of pS189 in human Ad293 cells. *Chem Res Toxicol* **11**, 211–216.

Mizzen CA, Cartel NJ, Yu WH, Fraser PE, McLaclan DR. 1996 Sensitive detection of metallothionein-1, -2 and -3 in tissue homogenates by immunoblotting: a method for enhanced membrane transfer and retention. *J Biochem Biophys Methods* **32**, 77–83.

Muller L. 1986. Consequences of cadmium toxicity in rat hepatocytes: mitochondrial dysfunction and lipid peroxydation. *Toxicology* **40**, 285–295.

Nakamura S, Kawata T, Nakayama A, Kubo K, Minami T, Sakurai H. 2004 Implication of the differential roles of metallothionein 1 and 2 isoforms in the liver of rats as determined by polyacrylamide-coated capillary zone electrophoresis. *Biochem Biophys Res Comm* **320**, 1193–1198.

Nordberg GF, Jin T, Nordberg M. 1994 Subcellular targets of cadmium nephrotoxicity: cadmium binding to renal membrane proteins in animals with or without protective metallothionein synthesis. *Environ Health Perspect* **102**, 191–194.

Palmiter RD. 1998 The elusive function of metallothioneins. *Proc Natl AcadSci USA* **95**, 8428–8430.

Perez MJ, Cederbaum AI. 2003 Metallothionein 2A induction by zinc protects HEPG2 cells against CYP2E1-dependent toxicity. *Free Radic Biol Med* **34**, 443–455.

Pourahmad P, O'Brien PJ, Jokar F, Daraei B. 2003 Carcinogenic metal induced sites of reactive oxygen species formation in hepatocytes. *Toxicol in Vitro* **17**, 803–810.

Prozialeck WC, Grunwald GB, Dey M, Reuhl KR, Parrish AR. 2002 Cadherins and NCAM as potential targets in metal toxicity. *Toxicol Appl Pharmacol* **182**, 255–265.

Rau W, Planas-Bohne F, Taylor DM. 1987 Influence of several chelating agents on the distribution and binding of cadmium in rats. *Hum Toxicol* **6**, 451–458.

Ren XY, Zhou Y, Zhang JP, Feng WH, Jiaco BH. 2003 Metallothionein gene expression under different time in testicular Sertoli and spermatogenic cells of rats treated with cadmium. *Reproductive Toxicol* **17**, 219–227.

Seglen PO. 1976 Preparation of isolated rat liver cells. *Methods Cell Biol* **13**, 29–83.

Shaikh ZA, Vu TT, Zaman K. 1999 Oxidative stress as a mechanism of chronic cadmium-induced hepatotoxicity and renal toxicity and protection by antioxidants. *Toxicol Appl Pharmacol* **145**, 256–263.

Shiraishi N, Hochadel JF, Coogan TP, Koropatnick J, Waalkes MP. 1995 Sensitivity to cadmium-induced genotoxocoty in rat testicular cells is associated with minimal expression of the metallothionein gene. *Toxicol Appl Pharmacol* **130**, 229–236.

Simpson IA, Yver DR, Hissin PJ, *et al*. 1983 Insulin-stimulated translocation of glucose transporters in the isolated rat adipose cells: characterization of subcellular fractions. *Biochim Biophys Acta* **763**, 393–407.

Tzirogiannis KN, Panoutsopoulos GI, Demonakou MD, *et al*. 2003 Time-course of cadmium-induced acute hepatotoxicity in the rat liver: the role of apoptosis. *Arch Toxicol* **77**, 694–701.

Vasconcelos MH, Tam SC, Hesketh JE, Reid M, Beattie, JH. 2002 Metal- and tissue-dependent relationship between metallothionein mRNA and protein. *Toxicol Appl Pharmacol* **182**, 91–97.

Von Zglinicki T, Edwall C, Ostlund E, Lind B, Norberg M, Ringertz NR, Wroblewski J. 1992 Very low cadmium concentrations stimulate DNA synthesis and cell growth. *J Cell Sci* 103, 1073–1081.

Waisberg M, Joseph P, Hale B, Beyersmann D. 2003 Molecular and cellular mechanisms of cadmium carcinogenesis. *Toxicology* **192**, 95–117.

Waku K. 1984 The chemical form of cadmium in subcellular fractions following cadmium exposure. *Environ Health Perspect* **54**, 37–44.

Wätjen W, Beyersmann D. 2004. Cadmium-induced apoptosis in C6 glioma cells: influence of oxidative stress. *Biometals* **17**, 65–78.

Wells WW, Seyfred MA, Smith CD, Sakai M. 1987 Measurement of subcellular sites of polyphosphoinositide metabolism in isolated rat hepatocytes. In Conn PM, Means AR, eds. *Methods in enzymology: Cellular Regulators Vol. 141*, part B, 92–99.

Wolstowski T, Krasowska A. 1999 Subcellular distribution of metallothionein and cadmium in the liver and kidney of bank voles (*Clethrionomys glareolus*) exposed to dietary cadmium. *Biometals* **12**, 173–179.

Zhou T, Zhou G, Song W, Eguchi N, Lu W, Lundin E, Jin T, Nordberg G. 1999 Cadmium-induced apoptosis and changes in expression of p53, *c-jun* and *MT-1* genes in testes and ventral prostate of rats. *Toxicology* **142**, 1–13.